

AD-A050 893

BATTELLE COLUMBUS LABS OHIO  
COMPUTATIONAL STUDY OF CHEMICAL REACTION DYNAMICS AT THE GAS-SO--ETC(U)  
NOV 77 G WOLKEN

F/G 7/4

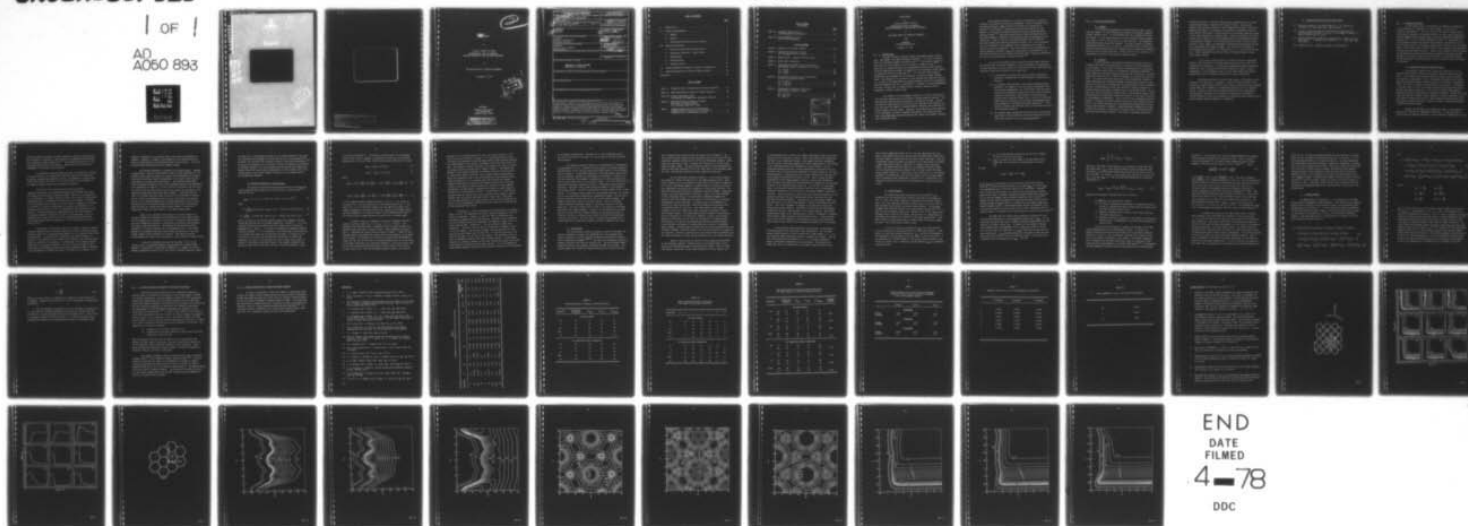
F49620-77-C-0004

UNCLASSIFIED

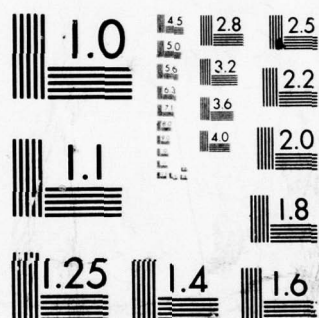
AFOSR-TR-78-0256

NL

1 OF 1  
AD  
A050 893



END  
DATE  
FILMED  
4-78  
DDC

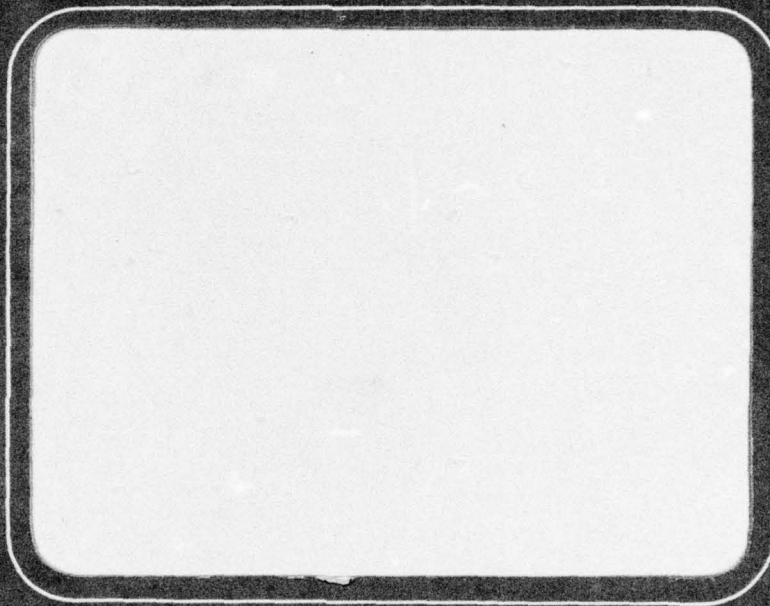


MICROCOPY RESOLUTION TEST CHART  
NATIONAL BUREAU OF STANDARDS-1963-A

AD A050893



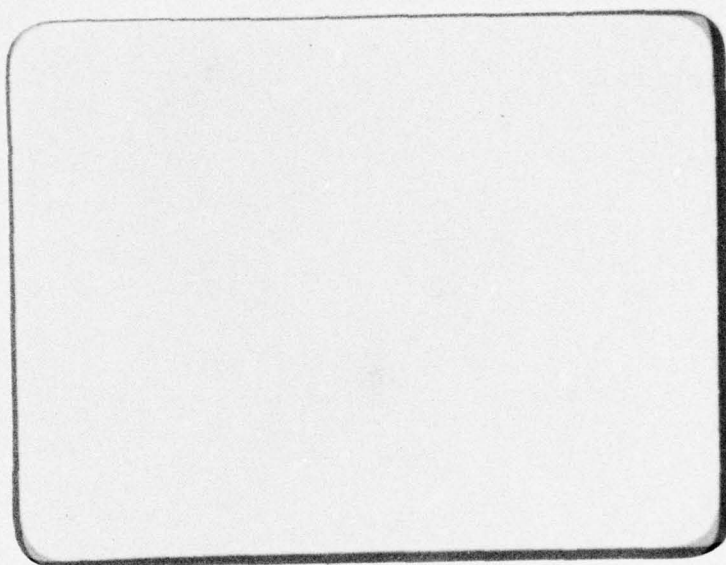
# Report



AD No.  
DDC FILE COPY



Approved for public release;  
distribution unlimited.



AIR FORCE OFFICE OF SCIENTIFIC RESEARCH (AFOSR)  
NOTICE OF TRANSMITTAL TO DDC  
This technical report has been reviewed and is  
approved for public release IAW AFR 190-12 (7)  
Distribution is unlimited.  
A. D. BLOSE  
Technical Information Officer



2

*Interim*  
**REPORT**

on

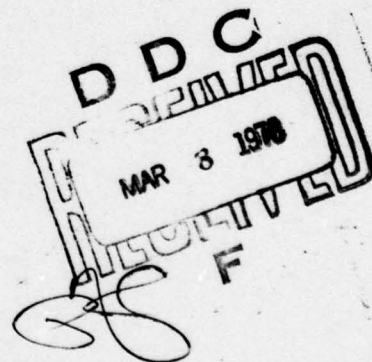
Contract F49620-77-C-0004

COMPUTATIONAL STUDY OF CHEMICAL  
REACTION DYNAMICS AT THE GAS-SOLID INTERFACE

to

AIR FORCE OFFICE OF SCIENTIFIC RESEARCH

November 10, 1977



BATTELLE  
Columbus Laboratories  
505 King Avenue  
Columbus, Ohio 43201

**DISTRIBUTION STATEMENT A**

Approved for public release;  
Distribution Unlimited

REPORT DOCUMENTATION PAGE		READ INSTRUCTIONS BEFORE COMPLETING FORM
1. REPORT NUMBER (18) AFOSR/TR-78-0256	2. GOVT ACCESSION NO.	3. RECIPIENT'S CATALOG NUMBER
4. TITLE (and Subtitle) 6 COMPUTATIONAL STUDY OF CHEMICAL REACTION DYNAMICS AT THE GAS-SOLID INTERFACE.		5. TYPE OF REPORT & PERIOD COVERED (9) Final rept., Interim
7. AUTHOR(s) (70) G/Wolken		6. PERFORMING ORG. REPORT NUMBER
9. PERFORMING ORGANIZATION NAME AND ADDRESS Battelle Columbus Laboratories Columbus, OH 43201		8. CONTRACT OR GRANT NUMBER(s) (15) F49620-77-C-0004
11. CONTROLLING OFFICE NAME AND ADDRESS AFOSR/NP Bolling AFB, Bldg.#410 Wash DC 20332		10. PROGRAM ELEMENT, PROJECT, TASK AREA & WORK UNIT NUMBERS (10) 2301 A5 61102F (17) A5
14. MONITORING AGENCY NAME & ADDRESS (if different from Controlling Office)		12. REPORT DATE (11) 19 Nov 77
		13. NUMBER OF PAGES 48 (12) 52 p.
		15. SECURITY CLASS. (of this report)
16. DISTRIBUTION STATEMENT (of this Report)  Approved for public release; distribution unlimited.		15a. DECLASSIFICATION/DOWNGRADING SCHEDULE
17. DISTRIBUTION STATEMENT (of the abstract entered in Block 20, if different from Report)		
18. SUPPLEMENTARY NOTES		
19. KEY WORDS (Continue on reverse side if necessary and identify by block number)		
20. ABSTRACT (Continue on reverse side if necessary and identify by block number) Using computer simulations an investigation was carried out describing the conditions under which a heterogeneously catalyzed reaction will enhance the deposit of energy into laser-active modes. The model describes the internal vibration-rotation states of diatomic molecules as they are formed and adsorbed from the surface. In addition an attempt is made to understand the particular features in the potential which lead to particular internal states.		

## TABLE OF CONTENTS

	<u>Page</u>
I. Project Aims . . . . .	1
II. Project Accomplishments. . . . .	3
A. Summary . . . . .	3
B. Details . . . . .	3
C. Publications Resulting from this Project. . . . .	5
III. Technical Discussion . . . . .	6
A. Overview of Gas-Phase Propensity Rules. . . . .	6
B. Interaction Potentials - Rigid Surface. . . . .	9
C. Calculations. . . . .	12
D. Moving Surface. . . . .	15
E. Graphite Surface. . . . .	19
IV. Pattern Recognition Approach to Classical Trajectories . . . . .	22
V. Quantum Calculations of Gas-Solid Energy Transfer. . . . .	23
References . . . . .	24

## LIST OF TABLES

Table I. Parameters Used in Generating the Various Potentials . . .	25
Table II. Mean Distribution of Energy in Product Molecules . . . . .	26
Table III. Product Vibrational State Distribution (%) Summed Over Rotational Sublevels. . . . .	27
Table IV. Mean Distribution of Energy in Product Molecules: (a) rigid surface; (b) 2 surface atoms free to move . . . . .	28
Table V. Binding energies (in eV) and equilibrium heights above the surface (in Å) for atoms at different sites on the graphite surface. . . . .	29



LIST OF TABLES  
(continued)

	<u>Page</u>
Table VI. Parameter values (in a.u.) for atom-graphite interactions. . . . .	30
Table VII. Morse parameters (in a.u.) for the H-H interaction . . . . .	31

LIST OF FIGURES

Figure 1. Geometry of the W(001) surface. . . . .	33
Figure 2. Equipotential contours (in eV) for the approach of H <sub>2</sub> to W(001). . . . .	34
Figure 3. Energy profiles along the reaction paths. . . . .	35
Figure 4. Basal plane of graphite . . . . .	36
Figure 5. Equipotential contours (in eV) for an atom approaching surface of graphite in (X,Y) plane	
(a) H atom . . . . .	37
(b) O atom . . . . .	38
(c) C atom . . . . .	39
Figure 6. Equipotential contours (in eV) for an atom in the (X,Y) plane of Figure 4	
(a) H (Z=1.9). . . . .	40
(b) O (Z=2.4). . . . .	41
(c) C (Z=1.8). . . . .	42
Figure 7. Equipotential contours (in eV) for H <sub>2</sub> approaching the graphite surface	
(a) Site "A" . . . . .	43
(b) Site "B" . . . . .	44
(c) Site "C" . . . . .	45

ACCESSION for	
NTIS	Write Section <input checked="" type="checkbox"/>
DDC	Buff Section <input type="checkbox"/>
UNANNOUNCED	<input type="checkbox"/>
JES T I C A T I O N	
BY	
DISTRIBUTION/AVAILABILITY CODES	
<div style="display: flex; justify-content: space-between;"> <span>11</span> <span style="font-size: 2em; font-family: cursive;">A</span> </div>	



FINAL REPORT

on

Contract F49620-77-C-0004

COMPUTATIONAL STUDY ON CHEMICAL  
REACTION DYNAMICS AT THE GAS-SOLID INTERFACE

to

AIR FORCE OFFICE OF SCIENTIFIC RESEARCH

from

BATTELLE  
Columbus Laboratories

November 10, 1977

I. Project Aims

Gas phase chemical reactions exhibit considerable energy specificity. For example, the highly exothermic reaction  $F + H_2 \rightarrow HF + H$  releases 67% of the available energy as vibration in HF.<sup>(1)</sup> This specific energy disposal has led to the construction of a variety of chemical lasers.<sup>(2)</sup> A great deal of research has gone into understanding precisely which features in the intermolecular potential are responsible for channeling a useful amount of energy into an active lasing mode.<sup>(3)</sup> It is now clear that large exothermicities are necessary but not sufficient to produce a useful chemical laser. The energy must be released in a very specific way during the reaction or, in spite of the large amount of energy available, most will be dissipated into non-lasing motions (e.g., translation). Therefore, not only exothermicity but also a certain type of "energy profile" along the reaction path is necessary to produce a useful laser.

The function of a heterogeneous catalyst is to alter the energy profile along the reaction path to accelerate a certain chemical reaction. This fact has multi-billion dollar importance to the American economy. However, altering the energy profile will not only alter the rate of the reaction but will also alter the details of energy disposal (including the possibility of energy disposal into the solid). Therefore, the primary aim of this research is to investigate, by means of computer simulations, the conditions under which a heterogeneously catalyzed reaction will enhance the deposit of energy into laser-active modes.

Using computer simulations, a study of the dynamics of reactions occurring at the gas-solid surface was undertaken. Battelle researchers had previously developed a model potential to describe the interaction of diatomic<sup>(4)</sup> and triatomic<sup>(5)</sup> gas molecules with solid surfaces, and had applied it to the case of hydrogen atoms and molecules interacting with a tungsten surface.<sup>(6)</sup> This model potential has a simple functional form so that rapid numerical evaluation of the potential and its derivatives can be carried out. Since it does not use pairwise additive forces, realistic gas-solid interactions including activation barriers, etc., can be simulated. It is also flexible in that parameters may be adjusted so as to model a variety of gas-solid potentials. Since the potential and its derivatives are easily evaluated, classical trajectory calculations of the dynamics of the gas-solid interaction can be computed and earlier work at Battelle demonstrated the utility of the method for a variety of cases.<sup>(6)</sup>

The aims of the present project involve using this model potential and the classical trajectory technique to study the dynamics of recombination of atoms adsorbed on a solid surface for a wide variety of gas-solid potentials. Questions of particular interest to the project are:

- (1) In endothermic reactions, what type of energy (vibrational, rotational, translational) is most effective in promoting the reaction?
- (2) In exothermic reactions what is the preferred energy disposal mechanism? For example, in the case under consideration here of atom-atom recombination on a solid surface, does the excess energy after recombination appear chiefly as product vibration, rotation or translation? What aspects of the interaction potential most sensitively affect this? How do the conclusions compare with the Polanyi rules for energy requirements and disposal mechanisms in gas-phase atom-diatom reactions?<sup>(7)</sup> What potential surfaces and conditions lead to vibrational excitation of the produce molecules?
- (3) The original model assumed that the atoms of the solid surface were fixed at their equilibrium positions during the reaction. Under what condition is this a good approximation?



## II. Project Accomplishments

### A. Summary

For a possible heterogeneously catalysed chemical laser, several steps are needed: (a) The reactants must adsorb on the surface, breaking internal chemical bonds. (b) The adsorbed atoms must recombine and leave the surface. (c) The reaction must occur under conditions where insignificant energy is lost to the solid (e.g., a fast reaction). (d) Significant energy should appear in product vibration. The past 12 months of research investigated questions (b), (c) and (d). As detailed below, we have found several conditions which seem to be necessary for the significant vibrational excitation of the product molecules. These conditions do not appear to be unreasonable and should be realizable in practical cases.

### B. Details

A model potential for gas-solid interactions has been used to investigate the dynamics of recombination of two atoms initially adsorbed on a solid surface. In the spirit of Polanyi's investigation into the effect of the potential energy surface on the dynamics of gas-phase reactions,<sup>(7)</sup> a range of gas-solid potential energy surfaces has been constructed. Classical trajectories have been used to study the dynamics of reactions on those surfaces. It has been found that many of the rules postulated by Polanyi for energy requirements and disposal mechanisms for gas-phase systems are applicable also to the case of recombination of adsorbed atoms to form a gas-phase molecule, notwithstanding the fact that additional reaction channels are possible having no gas-phase counterpart (e.g., the adsorbed state). We have found that repulsive potential surfaces which in the gas-phase require vibrational energy in the bond under attack for reaction, do not lead to reaction for heterogeneous recombination. This is true also for endothermic potential surfaces. Attractive potential surfaces give rise to more vibrational excitation in the product molecules and less translational energy than do mixed energy release surfaces. However, a light-heavy mass combination was found to remove the increase in vibrational excitation found in attractive rather than mixed energy release surfaces. The energy is channeled instead into

rotational excitation. The mixed energy release surfaces give rise to more translational energy, consistent with Polanyi's result. Previous work assumed a rigid surface providing a static background potential in which the adsorbed atoms moved. An extension of this model is described in which the rigid surface restriction is relaxed and one or more surface atoms are allowed to move interacting with the adsorbed atoms. Using this potential the rigid surface model is shown to be a good approximation for describing many aspects of recombination dynamics. Also, obtaining partial support from the present contract, a short project was undertaken to investigate more accurate methods for including gas-solid energy transfer. This project was undertaken in collaboration with Professor S. A. Adelman and Dr. Y. W. Lin of Purdue University. Useful information was obtained about the quantum dynamics of gas-solid energy transfer.

In the course of this research, it became clear that considerable computer time was wasted in following trajectories that did not lead to recombination and desorption. We investigated computerized pattern recognition methods as a way to pre-select only those trajectories likely to lead to recombination. Our preliminary results in this area indicate that pattern recognition could be an important time-saver in future calculations.

The above work (and all previous work) used a solid surface with the geometry of the (001) face of tungsten. A model potential suitable for the interaction of gas molecules with the basal plane of graphite has been developed and has been used to examine the recombination dynamics of  $H_2$  on a graphite surface. Results of this study are being prepared for future publication with particular reference to the mechanism of interstellar  $H_2$  formation (widely believed to occur on the surfaces of interstellar grains which spectroscopic evidence strongly suggests to be graphite).



C. Publications Resulting From This Project

- (1) "Pattern Recognition in Chemical Dynamics", J. H. McCreery and G. Wolken, Jr., Chem. Phys. Lett., 46, 469 (1977).
- (2) "A Test of the First Order Distorted Wave Born Approximation in Gas-Solid Energy Transfer", Y. W. Lin, S. A. Adelman, G. Wolken, Jr., Surface Science, 66, 376 (1977).
- (3) "Atomic Recombination Dynamics on Solid Surfaces: Effect of Various Potentials", J. H. McCreery and G. Wolken, Jr., J. Chem. Phys., 67, 2551 (1977).
- (4) "Formation of H<sub>2</sub> on Graphite Surfaces" (in preparation).

### III. Technical Discussion

In the present study, we investigate the dynamics of recombination of two atoms initially adsorbed on a solid surface. In the spirit of Polanyi's investigation<sup>(7)</sup> into the effect of the potential energy surface on the reaction dynamics for gas-phase systems, we used a range of gas-solid potential energy surfaces generalizing our previous studies of recombination dynamics.<sup>(6a,b)</sup> Also, we present preliminary results for heterogeneous reaction dynamics in which the surface atoms themselves are permitted to move. For the cases studied, no significant changes result from motion of the surface atoms. Section III-A gives a brief overview of the propensity rules developed by Polanyi for gas-phase collisions. Section III-B reviews the model potential for gas-surface collisions and describes the range of potentials used here. Section III-C presents results and discussion for the rigid surface model. The generalization to a moving surface is given in Section III-D, and results are presented.

#### A. Overview of Gas-Phase Propensity Rules

For exothermic reactions  $A+BC \rightarrow AB+C$  with exothermicity in the range 30-50 kcal mole<sup>-1</sup> and activation barriers typically around a few kcal mole<sup>-1</sup>, it was shown that attractive potential surfaces, where the energy is released as A approaches B, lead to vibrational excitation of the product molecules; repulsive surfaces, where the energy is released as AB separates from C, give rise to rotation and translation of the products. An exception to this was found to occur for repulsive surfaces when the attacking atom A was very much heavier than atom C. This leads to "mixed energy release" dynamics and product vibrational and rotational excitation. Complex collisions, where more than one encounter between reagents or products takes place, were also found to deviate from the rule. Such secondary encounters mainly occur on attractive surfaces and tend to reduce the product vibrational excitation on highly attractive surfaces.

Polanyi and co-workers also examined the effect of the position of the crest of a barrier for thermoneutral reactions. It was found that "a barrier along the approach coordinate is most efficiently surmounted by motion

along the approach coordinate (reagent translation) whereas a barrier along the coordinate of separation is most efficiently surmounted by motion along that coordinate (reagent vibration)".<sup>(7)</sup> The converse was found to be true for energy hollows rather than barriers. These effects were found to be independent of the masses of the particles.

For endothermic reactions where the crest of the barrier is located in the exit valley, it was found that vibrational energy in the bond under attack was necessary for successful reaction. An exception to this was when C had a much smaller mass than A or B, in which case too much vibration in the reagents markedly reduced the probability of reaction.

These results were concluded from series of classical trajectory calculations on London-Eyring-Polanyi-Sato<sup>(8)</sup> (LEPS) type potential functions for gas-phase triatomic systems. The aim of the present work is to investigate in a similar manner the effect of the form of the potential energy function on the dynamics of reactions on solid surfaces. Reactions on solid surfaces can be thought of in three steps: (1) adsorption of the gas on the solid; (2) possible equilibration, or partial equilibration of the adsorbed particles with the solid; (3) recombination and desorption of a gas molecule. If the adsorption and recombination steps are fast compared to the adsorbate-lattice relaxation time, step 2 can be neglected. The circumstances under which this occurs are the circumstances under which the rigid surface model should be applicable. This is discussed more fully in Section III-D.

The purpose of the present study is to attempt to model the internal vibration-rotation states of diatomic molecules as they are formed and desorb from the surface and to understand which features in the potential lead to what internal states. As Polanyi first discussed for gas-phase exothermic reactions<sup>(9)</sup>, circumstances exist in which useful amounts of the reaction energy appear as vibration in the products. A further goal of the present computer simulations is to explore (admittedly, in a very crude way) possible situations under which similarly useful vibrational populations might be obtained from heterogeneously catalyzed reactions. The function of a catalyst is to



change the energetics of the reaction path to accelerate the formation of products. Similarly, a change in the energetics of the reaction path will affect the distribution of the available energy in the products. It is this modified energy distribution we will attempt to model.

We envision attempting to simulate the following process: consider a (hypothetical) reaction of gas molecules that is highly exothermic but, for whatever reason, does not produce the desired state distribution of products. A catalyst is used that alters the energetics of the reaction path and produces some other product state distribution. The available energy comes from the gas-phase reagents with the solid remaining chemically and dynamically inert throughout the reaction. (We will relax the restriction that the solid be strictly rigid in Section III-D, but we will assume that virtually all the available energy comes from the gas-phase reagents. The extent that the solid is an energy sink under these conditions will be discussed in Section III-D.) While the temperature of the solid can often affect its catalytic activity, it is usually assumed that the primary mechanism is that of a hot surface effectively lowering activation barriers more than a cold surface. Since this does not require gas-surface energy transfer, it too can be treated with either the rigid surface or the moving surface model.

Hence, we are concerned with basically a two-step process: adsorption followed by recombination and desorption with a net energy release into the products and, possibly into the solid. The present work considers only the recombination processes to assess how the potential surface affects the product state distributions. The dynamics of the adsorption process determine the initial conditions for the recombination (i.e., the initial momenta of the adsorbed atoms when they collide) and therefore is one step further removed from the formation of products. The effect of various initial momenta on product state distributions is the subject of a future study.

We have also considered the question: how many, if any, of the "Polanyi rules" for gas-phase dynamics are applicable also to gas-surface dynamics, in particular to recombination dynamics? For example, in an exothermic recombination reaction is it true that an attractive potential surface



will give rise to vibrational excitation of the product molecule? The potential functions used throughout this work have the form of the modified LEPS potential that has been used in previous studies of gas-solid interactions.<sup>(3-7)</sup> By varying the parameters in the potential function we generate a wide variety of potential surfaces. We use both equal mass and unequal mass combinations. We have relaxed the rigid surface approximation in part allowing some of the surface atoms to move, and we examine the effect of the surface motion on the recombination dynamics.

### B. Interaction Potentials - Rigid Surface

The potential functions used were generated from the diatom-solid surface modified LEPS potential that has been used in previous work.<sup>(4-6)</sup> This has the form

$$V_{\text{LEPS}} = U_1 + U_2 + U_3 - [A_1^2 + (A_2 + A_3)^2 - A_1 (A_2 + A_3)]^{\frac{1}{2}} \quad (1)$$

where

$$U_i = \frac{D_i}{4(1+\Delta_i)} \left[ (3+\Delta_i) \exp(-2\alpha_i(r_i-r_{i0})) - (2+6\Delta_i) \exp(-\alpha_i(r_i-r_{i0})) \right] \quad (2)$$

$$A_i = \frac{D_i}{4(1+\Delta_i)} \left[ (1+3\Delta_i) \exp(-2\alpha_i(r_i-r_{i0})) - (6+2\Delta_i) \exp(-\alpha_i(r_i-r_{i0})) \right] \quad (3)$$

and  $D_i$ ,  $\alpha_i$ , and  $r_{i0}$  are the dissociation energy, Morse parameter and equilibrium distance for the  $i$ th two-body interaction. We take  $i = 1$  to be the atom-atom interaction and assume a typical  $H_2$  Morse curve to obtain the parameters  $D_1$ ,  $\alpha_1$  and  $r_{10}$ .  $\Delta_i$  is used as a parameter to generate different potential surfaces.  $i = 2, 3$  correspond to the atom-surface interactions and it is assumed that these are the same for both atoms. To account for the structure of the solid in the atom-surface interactions we require the parameters  $D$ ,  $\alpha$  and  $r_0$  to be functions of  $x$  and  $y$ , where the  $x$ - $y$  plane is parallel to the plane of the solid surface. The symmetry assumed for the surface is that of the (100) face of a bcc solid and the geometry is that

of tungsten (see Figure 1). Following the previous work of  $H_2$  interacting with the (100) face of tungsten, we assume the existence of three possible binding sites, the on-top (1CN), bridge (2CN) and hole (5CN) sites. We take

$$D(x,y) = D_0 [1 + \delta Q(x,y)] \quad (4)$$

$$r_o(x,y) = Z_m [1 + \epsilon P(x,y)] \quad (5)$$

where

$$Q(x,y) = k \left[ \cos \left( \frac{2\pi x}{a} \right) + \cos \left( \frac{2\pi y}{a} \right) \right] - A \left[ \cos \left( \frac{2\pi x}{a} \right) - 1 \right] \left[ \cos \left( \frac{2\pi y}{a} \right) - 1 \right] \quad (6)$$

$$P(x,y) = k \left[ \cos \left( \frac{2\pi x}{a} \right) + \cos \left( \frac{2\pi y}{a} \right) \right] - B \left[ \cos \left( \frac{2\pi x}{a} \right) - 1 \right] \left[ \cos \left( \frac{2\pi y}{a} \right) - 1 \right] \quad (7)$$

$a$  is the tungsten nearest neighbor distance ( $=5.97$  a.u.).  $k$  is chosen to be either 0 or 1; in the previous work it was always assumed to be 1. The effect of  $k = 0$  is to introduce channels into the egg-carton shape of the surface by making the on-top and bridge sites identical for hydrogen binding. The Morse parameter  $\alpha$  is chosen as before to be  $\left[ 0.02894/D(x,y) \right]^2$  where  $D$  is in atomic units of energy giving  $\alpha$  in atomic units of inverse length.

We have a total of 9 parameters with which to generate different potential surfaces, namely  $D_0$ ,  $\delta$ ,  $k$ ,  $A$ ,  $Z_m$ ,  $\epsilon$ ,  $B$ ,  $\Delta_1$ ,  $\Delta(=\Delta_2=\Delta_3)$ . The parameters were adjusted to give 9 different potential energy surfaces with varying barriers and modes of energy release. These parameters are given in Table I. Equipotential contour plots are given in Figure 2. These are for a hydrogen molecule approaching the surface with the axis parallel to the plane of the surface. The mid-point of the bond is perpendicularly approaching a bridge (or 2CN) site and the bond is stretching symmetrically in the direction of the atomic adsorption site of greatest stability. This is the on-top (1CN) site for all the potential surfaces except IX where the hole site (5CN) is the most stable site. With the coordinate system of Figure 1, the bond in

potential IX is stretching parallel to the x axis along the line  $y = a/2$ , while for the other potential surfaces, it is stretching along the y axis. The dashed line indicates the minimum energy reaction path from the reactants, two atoms adsorbed on the surface, to products, a molecule far from the surface. The X marks the initial position of the atoms in the 1CN or 5CN sites. The energy along the reaction path is shown in Figure 3. The dashed line parallel to the ordinate indicates the position along the reaction path of an arbitrarily defined "transition state" between reactants and products. While this transition state is not well-defined for these molecule-surface potential functions, it is a concept useful for defining the boundary between entrance and exit channels and therefore plays a role in any discussion of the effects of barrier position in relation to these channels. Consequently, we have chosen to determine the transition state region approximately for each potential surface. In potentials IV, V, and VIII the distance along the reaction path of the transition state region is easily defined since the reaction path makes quite a sharp turn at that point. For the other potentials, the exact position is not clearly defined but we chose it to be approximately half-way around the curve in the reaction path in the transition state region.

Potentials I - III are endothermic with endothermicity of approximately 1.26 eV. We assume that the overall reaction catalyzed by the solid surface is exothermic. However, it may occur that the adsorption step releases more energy than the total reaction. Therefore, the recombination will occur between atoms with considerable translational energy, but on an uphill reaction path. Potentials I - III are intended to model this possibility. Potential I has the crest of the barrier (of height 1.39 eV) in the exit channel. The on-top and bridge sites are identical for this case and are more stable than the hole site. II also has the crest of the barrier (of height 1.39 eV) in the exit channel. The adsorption sites, in order of decreasing stability are on-top, bridge and hole. For gas-phase reactions on potential surfaces of this form, vibrational energy in the bond under attack is necessary for successful reaction. It is not immediately obvious what analogous condition on the gas-solid potentials will be necessary



for successful recombination. Potential III is also endothermic but has the crest of the barrier (of height 1.99 eV) at more or less the transition state position.

The remaining potential functions are exothermic with exothermicity of approximately 1.73 eV. Potential IV has no barrier to molecule formation and desorption, and the energy release occurs about equally in both entrance and exit channels. For gas-phase reactions, this mixed energy release would lead to vibration, rotation and translation of the products. Potential IV also has no barrier from reagents to products but for this case much of the energy release takes place in the entrance channel. This is an attractive surface and for gas-phase systems would lead to vibrationally excited product molecules. Potential VI has a small barrier of height 0.10 eV entirely in the entrance channel. As with IV about half the energy release occurs in each channel. If an analogy can be drawn with the gas-phase reactions, the barrier will be most efficiently surmounted by translational energy. VII also has a barrier (of height 0.33 eV) with crest just in the entrance channel. The energy release occurs mostly in the exit channel. This is a repulsive surface requiring vibrational energy for successful reaction in the gas-phase case. VIII has no barrier and, as with V, has nearly all the energy released in the entrance channel. Potential IX is generated from the same data as VI except that the relative stability of the adsorption sites is reversed, the hole site being the most stable followed by the bridge and then the on-top sites. This also leads to a mixed energy release type of surface when the two atoms are initially positioned at adjacent hole sites.

### C. Calculations

For each potential surface we computed a series of classical trajectories designed to simulate the recombination of two adsorbed atoms. Initial conditions for those trajectories have been described in previous work on recombination dynamics.<sup>(6a,b)</sup> The atoms were positioned initially at adjacent 1CN sites (5CN sites for potential IX). The total initial kinetic energy was fixed but was randomly distributed between the two atoms. The initial momenta were chosen with random directions but restricted so the x



and y components were directed within the square shown in Figure 1. The total initial kinetic energy for the system was chosen to be 3.50 eV for the endothermic potential surface and 0.50 eV for the exothermic surfaces. These values are sufficiently large to surmount any barriers and to allow a wide range of product states. For each potential surface we ran trajectories for atoms of equal mass (hydrogen) and for one light (mass 1) and one heavy (mass 80) atom. Three-hundred trajectories were computed for each case.

For the endothermic potential surfaces I - III, very few molecules were formed for either the equal mass or the light-heavy mass cases. Thus, without running a very large number of trajectories (as was done in Reference 6,7) we have insufficient numbers of product molecules to draw any statistically meaningful conclusions about properties of the product molecules. For successful gas-phase reactions on endothermic potential surfaces, vibrational energy in the bond under attack is necessary. There is no direct analogue of this vibrational energy in the gas-solid recombination dynamics but motion on the solid surface does not appear to be sufficient for successful recombination on such potentials. Of course, even a low probability of reaction per collision may lead to molecule formation and desorption after a sufficient number of collisions. This would require a much longer residence time on the surface and, hence, a greater possibility for gas-solid energy transfer. Such equilibration with the surface is inconsistent with the constraints of our model and, therefore, actually running large numbers of trajectories is not likely to contribute to an understanding of the processes. We conclude that endothermic desorption processes appear to be relatively inefficient at forming molecules, even with considerable kinetic energy. Increased energy transfer with the solid is expected and hence increased "leakage" of reaction energy on the way from reactants to products is also expected. Therefore, reactions with very strongly bound intermediates are not likely candidates to channel energy efficiently into the product molecules.

Tables II and III give the results of the trajectory calculations on the exothermic surfaces. Potential VII is not included since in this case also an insufficient number of molecules were formed. This is a repulsive surface, having most of the energy released in the exit channel, and

in the gas-phase such a surface also requires vibrational energy in the bond under attack for successful reaction. While there seems to be no gas-solid analogue to such vibrational energy, we have again found that translation over the surface (including components of motion perpendicular to the surface) is not sufficient despite the exothermicity of the reaction. For the remaining exothermic potential surfaces approximately one-third of the trajectories led to reaction and the formation of a product molecule. The total energy available to these molecules for internal excitation (including zero-point energy) and translation is about 2.25 eV. Table II gives the mean distribution of this energy between vibration, rotation and translation. Table III gives the vibrational state distributions summed over the rotational sublevels of the desorbed product molecules. For the case of two hydrogen atoms, the attractive potential surfaces V and VIII lead to considerable vibrational excitation, as is the case for attractive surfaces in gas-phase reactions. These surfaces also lead to the most rotational excitation of the products (and hence the least translational energy, consistent with the attractive potential surfaces). Potential IV is a mixed energy release surface and leads to just about equal amounts of energy in vibration and translation. This can be regarded as analogous to the gas-phase results for mixed energy release surfaces. Potentials VI and IX are also mixed energy release but each has a small barrier in the entrance channel. The initial translational energy of the adsorbed atoms is seen to be adequate to surmount these barriers, again consistent with gas-phase results. VI and IX differ only in the relative ordering of the adsorption sites and this difference seems to have little effect on the recombination properties of the surfaces.

The light-heavy mass combination has the effect of smoothing out the sharper peaks in the vibrational state distribution. For the mixed energy release potentials IV and VI (which for  $H_2$  peak around  $v = 1$ ,  $v = 2$ ) this causes the mean vibrational energy to increase very slightly. For the other potentials which peak around  $v = 2$ ,  $v = 3$ , the mean vibrational energy is decreased considerably by this smoothing. The proportion of energy that occurs as translation of the product molecules varies little



with the mass combination except for IX. For the light-heavy case this means a much smaller velocity of the molecule and indeed these trajectories took much longer to compute than did the equal (light) mass case. Since the translational energy is roughly the same for the two mass cases, the change in mean vibrational energy is reflected in a change in mean rotational energy. The unequal mass case gives rise to increased rotational energy for the attractive potentials surfaces V and VIII and also for the mixed energy release surface IX. Potentials VI and IX differ only in the relative ordering of the adsorption sites and give similar results for equal masses, but for light-heavy mass combinations IX gives rise to significantly less vibrational excitation than VI and correspondingly more rotation and translation.

#### D. Moving Surface

The rigid surface model was previously justified<sup>(4)</sup> by the assumption that the adsorbed atoms encounter each other and recombine (or not) on a time scale short compared to adsorbate-lattice energy transfer times. For light adsorbates and heavy surface atoms, it was felt that the mass difference would ensure only modest energy transfer. Our previous estimates were 2% energy transfer for H atom-tungsten interactions,<sup>(6b)</sup> or about 4% for H<sub>2</sub>-tungsten interactions. However, since we are using heavier adsorbate atoms in some of the present calculations, it is appropriate to investigate more carefully the validity of the rigid surface model. Therefore, we have run trajectories with the rigid surface restriction relaxed and some of the surface atoms allowed to move.

It is first necessary to generalize  $V_{LEPS}$  (the LEPS potential for the interaction of a gas molecule with a rigid solid surface). In addition to a gas-rigid surface interaction,  $V_{LEPS}$  can also be considered as the interaction of a gas molecule with the lattice sites of the solid. If we allow motion of the solid atoms, at any instant those atoms may or may not be at a lattice site. Therefore, we have modified  $V_{LEPS}$  by introducing correction terms:



- (1)  $V_R$ , the restoring force on each atom of the solid, tending to return it to its lattice site;
- (2)  $V_{CORR}$ , to account for the change in the gas-surface interaction when the solid atom is displaced from its lattice site.

We have

$$V_{total} = V_{LEPS} + V_R + V_{CORR} \quad (8)$$

$V_R$  and  $V_{CORR}$  must vanish when all the solid atoms occupy their lattice positions. We have used pair-potentials for  $V_R$  and  $V_{CORR}$  to correct  $V_{LEPS}$  in an approximate way to allow for motion of the solid atoms. Assuming that  $V_R$  binds the solid atom to its lattice site constitutes an Einstein model of the solid. Certainly, pairwise atom-atom interactions can be used for  $V_R$ , and are commonly used to simulate properties of bulk solids<sup>(10)</sup>. However, we feel that the simplicity of the Einstein model, and the corresponding savings of computer time, is justified for the present rough estimates of energy transfer. More refined energy transfer calculations, using a generalized Langevin oscillator model for the solid, demonstrate that the Einstein model is a reasonable first approximation for short collision times.<sup>(11)</sup>

The model does not include the non-additive corrections for the solid-solid interactions, or the non-additive corrections to  $V_{CORR}$ . For the restoring force  $V_R$  we have used a harmonic potential binding an atom of the solid to its (fixed) lattice site. To account for the change in the gas-solid potential due to displacement of the surface atom from its lattice site, we have used a pair-potential for  $V_{CORR}$  connecting each gas atom with each surface atom.  $V_{LEPS}$  already contains the interaction of each gas atom with each lattice site, so to avoid including it twice, this lattice site interaction must be subtracted from  $V_{CORR}$ . We take

$$V_{\text{CORR}} = \sum_g^{N_g} \sum_s^{N_s} \left[ W(R_{g-s}) - W(R_{g-l}) \right] \quad (9)$$

Where  $N_g$  is the number of gas atoms,  $N_s$  is the number of solid atoms that are free to move,  $R_{g-s}$  is the distance between the gas atom and the solid atom and  $R_{g-l}$  is the distance between the gas atom and the lattice site of the solid atom. As required, if the surface atom occupies its lattice site,  $R_{g-s} = R_{g-l}$  and  $V_{\text{CORR}} = 0$ . The total gas-solid potential for the moving surface case is

$$V_{\text{total}} = V_{\text{LEPS}} + \sum_s^{N_s} V_R^s + \sum_g^{N_g} \sum_s^{N_s} \left[ W(R_{g-s}) - W(R_{g-l}) \right] \quad (10)$$

where  $V_R^s$  is the harmonic restoring force for solid atom  $s$ .

To summarize, the revised model includes:

- (1) all forces, pairwise and non-pairwise, to describe the interaction of a gas molecule with a surface when the surface atoms are fixed at their lattice sites.
- (2) pairwise corrections for the motion of the solid atoms away from their lattice sites.
- (3) pairwise corrections to account for the change in the gas-solid potential due to displacement of the surface atoms from their lattice sites.

We have used this potential to examine the validity of the rigid surface approximation for the recombination studies. We require the harmonic restoring force for the solid atoms, and the gas-solid atom Morse potential ( $W$  in Eq. 9). For the harmonic restoring force we need an estimate of the Einstein temperature of the surface. The Einstein temperature can be estimated from the Debye temperature either by requiring the best single-oscillator approximation to the Debye mode density<sup>(11)</sup> or by expanding the high temperature Debye and Einstein heat capacities and matching terms

through  $T^{-2}$ . In both cases, one finds the Debye temperature to be smaller than the Einstein temperature by a factor of  $\sqrt{0.6}$ . Also, in order to correct approximately for the smaller Debye temperature of the surface compared to the bulk, an extra factor of  $(2/3)$  is used<sup>(13)</sup>. Hence,

$$\theta_{\text{Einstein}}^{(\text{surface})} = (2/3)\sqrt{0.6} \theta_{\text{Debye}}^{(\text{bulk})} \quad (11)$$

Using  $\theta_{\text{Debye}}^{(\text{bulk})} = 400^\circ\text{K}$  yields  $\theta_{\text{Einstein}}^{(\text{surface})} = 210^\circ\text{K}$ . This gives a harmonic force constant for a tungsten solid atom of 0.074 a.u. The solid atoms were assumed initially to be at their equilibrium positions and those that were free to move were given an initial kinetic energy (the same for all the atoms) equal to the average energy of the harmonic oscillator at a surface temperature of  $300^\circ\text{K}$  with an Einstein temperature of  $210^\circ\text{K}$ . Then each solid atom initially has kinetic energy of 0.00197 a.u.; the initial direction of velocity of the atoms was randomly chosen so that there was equal probability of it being within any differential solid angle. The gas-solid Morse potential used in  $V_{\text{CORR}}$ ,  $W(R_{\text{g-s}})$ , was chosen to have  $\alpha = 0.5123$  a.u.;  $D = 0.055$  a.u. and  $r_0 = 3.12$  a.u. These parameters correspond to the hydrogen atom-tungsten 1CN Morse potential used previously.<sup>(3)</sup>

To examine the validity of the rigid surface model in recombination dynamics, 100 trajectories were computed for each of potentials IV, V, VI, and VIII and for both the equal (light) mass and the light-heavy mass combination. The initial conditions of the adsorbed gas atoms were chosen to be the same in these trajectories as in the first 100 trajectories for those potentials in the rigid surface model. Two surface atoms were allowed to move, those being the two atoms in the 1CN sites directly below the adsorbed gas atoms in their initial configuration. The initial directions of velocity of these two surface atoms were randomly selected. Table IV shows a comparison of the results of these trajectories for the rigid surface and for the moving surface cases. It is not clear why the moving surface atoms seem to increase the total probability of molecule formation by a



factor of two. The energy transferred between the gas atoms and the surface atoms for both the equal and unequal mass cases was, in the mean, 6 - 7% of the total energy available to the product molecules. The mean distribution of the available energy among vibration, rotation and translation is changed very little by the motion of the surface. More work is needed to assess carefully the role of surface motion on angular distributions (which measure momentum transfer and are frequently a more sensitive probe of collision dynamics) as well as the interaction of surface atoms and adsorbate atoms with comparable masses. The generalized Langevin oscillator model of Adelman and Doll<sup>(12)</sup> could be included to mimic the effects of the full lattice on the reaction zone. The present studies indicate that the product state distributions of recombining atoms are not very sensitive to the motion of the surface atoms.

#### E. Graphite Surface

The LEPS potential in Equations 1 - 3 is suitable for any diatom-solid system with appropriate input parameters. The symmetry of the tungsten surface used is reflected in the functional forms of the atom-surface Morse parameters given in equations 4 - 7. Those functional forms are appropriate for any solid surface of square symmetry. To study the basal plane of graphite (see Figure 4) we require  $D_o$ ,  $\alpha$ , and  $r_o$  to be functions of hexagonal symmetry. Once more taking the x-y plane parallel to the plane of the surface, suitable functional forms are:

$$\begin{aligned}
 D_o = & a + \frac{b}{3} \left\{ \cos(\beta R_{a1}) + \cos(\beta R_{a2}) + \cos(\beta R_{a3}) + \cos(\beta R_{b1}) + \cos(\beta R_{b2}) \right. \\
 & + \cos(\beta R_{b3}) + \cos(\beta R_{a1}) \cos(\beta R_{b1}) + \cos(\beta R_{a2}) \cos(\beta R_{b2}) \\
 & \left. + \cos(\beta R_{a3}) \cos(\beta R_{b3}) \right\} + \frac{c}{3} \left\{ \left[ \cos^2(\beta R_{a1}) - 1 \right] \left[ \cos^2(\beta R_{b1}) - 1 \right] \right. \\
 & \left. + \left[ \cos^2(\beta R_{a2}) - 1 \right] \left[ \cos^2(\beta R_{b2}) - 1 \right] + \left[ \cos^2(\beta R_{a3}) - 1 \right] \left[ \cos^2(\beta R_{b3}) - 1 \right] \right\}
 \end{aligned} \tag{12}$$

and

$$\begin{aligned}
 r_o = d + \frac{e}{3} \{ & \cos(\beta R_{a1}) + \cos(\beta R_{a2}) + \cos(\beta R_{a3}) + \cos(\beta R_{b1}) + \cos(\beta R_{b2}) \\
 & + \cos(\beta R_{b3}) + \cos(\beta R_{a1}) \cos(\beta R_{b1}) + \cos(\beta R_{a2}) \cos(\beta R_{b2}) \\
 & + \cos(\beta R_{a3}) \cos(\beta R_{b3}) \} + \frac{f}{3} \{ [\cos^2(\beta R_{a1}) - 1][\cos^2(\beta R_{b1}) - 1] \\
 & + [\cos^2(\beta R_{a2}) - 1][\cos^2(\beta R_{b2}) - 1] + [\cos^2(\beta R_{a3}) - 1][\cos^2(\beta R_{b3}) - 1] \}
 \end{aligned} \quad (13)$$

where

$$\begin{aligned}
 R_{a1} &= -y - \frac{x}{\sqrt{3}} & R_{b1} &= \frac{2x}{\sqrt{3}} \\
 R_{a2} &= \frac{x}{\sqrt{3}} - y & R_{b2} &= \frac{x}{\sqrt{3}} + y \\
 R_{a3} &= \frac{2x}{\sqrt{3}} & R_{b3} &= y - \frac{x}{\sqrt{3}}
 \end{aligned}$$

and  $\beta = (2\pi)/(s\sqrt{3})$  where  $s$  is the graphite nearest neighbor bond distance ( $= 2.68$  a.u.). The parameters  $a$ ,  $b$ ,  $c$ ,  $d$ ,  $e$ , and  $f$  are dependent on the particular atom-graphite interaction. For H, O, and C on graphite they have been chosen by fitting the above functional forms to binding energies and equilibrium heights above the surface for each atom in bridge, on-top and hole sites above the graphite surface. Those sites are shown in Figure 4. The values used for the binding energies above the surface were taken from semi-empirical calculations by Bennett et. al.<sup>(14)</sup> and Hayns<sup>(15)</sup> with the binding energies scaled to 0.2 of the calculated values as these authors suggest. Table V gives these scaled values. The resulting parameter values are given in Table VI. The Morse parameter  $\alpha$  for the atom-graphite interactions was chosen by fitting the potential energy curve in the region of the minimum at one of the binding sites to parabola in the  $z$  direction; this gives

$$\alpha = \sqrt{\frac{\alpha_0}{D_0}} \quad (14)$$

where  $D_0$  is in a.u. and  $\alpha_0 = 0.10585$  for H, 0.12603 for O, and 0.1392 for C on graphite. Figures 5,6 are plots of H, O, and C atoms above the basal plane of graphite.

For  $H_2$  + graphite the potential is of the form given by equations 12, 13. The values of the Morse parameters used for the  $H_2$  potential are given in Table VII. The Sato parameters were all chosen equal to 0.0. Plots of the  $H_2$  + graphite potential are shown in Figure 11. Studies were begun on the recombination dynamics of two hydrogen atoms adsorbed on a graphite surface.



#### IV. Pattern Recognition Approach to Classical Trajectories

Previous work done at Battelle on the recombination dynamics of adsorbed atoms, had required the calculation of very large numbers (~20,000) of classical trajectories. This was because in about 97% of the trajectories computed the adsorbed atoms did not combine and desorb to form a gas-phase molecule but remained adsorbed on the surface for the duration of the trajectory. The use of pattern recognition in conjunction with classical trajectories was investigated as a possible method of avoiding the computation of very large numbers of trajectories.<sup>(16)</sup> In brief, a small sample of the previously calculated trajectories were used to "train" the pattern recognition program to predict in which of the trajectories (not in the selected sample) the atoms would recombine to form a molecule and would therefore be of interest to compute, and in which trajectories the atoms would remain adsorbed on the surface. The computation of a trajectory involves:

- (1) choosing a set of initial conditions, and
- (2) integrating the classical equations of motion from the initial conditions to some end point

Since the equations of motion are the same for all the trajectories that simulate the same system, the outcome of any are trajectory must depend only on the particular initial conditions selected for that trajectory. Using pattern recognition techniques we have attempted to predict the outcome of a trajectory from just the initial conditions.

Two different methods of pattern recognition were used, the nearest neighbor method<sup>(17)</sup> and an adaptive digital learning network.<sup>(18)</sup> Prediction accuracy of about 80% was found to be obtainable at a savings in computer time over integrating the trajectories of a factor of 500 for the nearest neighbor method and of 100 for the digital learning network. The method promises to be very useful in chemical dynamics. The method was not applied in any of the other cases reported here since only 100 trajectories were computed for each set of fixed initial conditions.

## V. Quantum Calculations of Gas-Solid Energy Transfer

In order to understand in detail the dynamics of gas-surface interactions, the energy transfer between the gas and the solid must be included. We have seen above how this can be built into our classical trajectory model, but for an accurate "benchmark" a quantum method is needed. In collaboration with scientists at Purdue University, and building on work previously done at Battelle, a test of a simple quantum approximation was undertaken.<sup>(19)</sup> As discussed in detail in Reference (19), simple quantum theories seem to work quite well for a substantial range of gas and solid temperatures.

### References

1. K. L. Kompa, "Chemical Lasers" (Springer-Verlag, Berlin, 1973).
2. R.W.F. Gross and J. F. Bott, "Handbook of Chemical Lasers", (Wiley, N.Y., 1976).
3. See "Features of Potential Energy Surfaces and their Effect on Collisions", by P. J. Kuntz in "Dynamics of Molecular Collisions - Part B", ed. W. H. Miller (Plenum, New York, 1976).
4. J. H. McCreery and G. Wolken, Jr., J. Chem. Phys. 63, 2340 (1975).
5. J. H. McCreery and G. Wolken, Jr., J. Chem. Phys. 66, 2316 (1977).
6. J. H. McCreery and G. Wolken, Jr., (a) J. Chem. Phys. 63, 4072 (1975), (b) 64, 2845 (1976), (c) 65, 1310 (1976), (d) Chem. Phys. Letters 39, 478 (1976), (e) Chem. Phys. 17, 423 (1976).
7. For a review see J. C. Polanyi, Acc. Chem. Res. 5, 161 (1972).
8. For a review see H. S. Johnston, "Gas Phase Reaction Rate Theory", (Ronald, New York, 1966) pp. 171-173 and references cited therein.
9. J. C. Polanyi, J. Chem. Phys. 34, 347 (1961).
10. See, for example, "Interatomic Potentials and Simulations of Lattice Defects", P. C. Gehlen, J. R. Beeler, Jr., R. I. Jaffee, eds. (Plenum Press, New York, 1972).
11. B. J. Garrison and S. A. Adelman, Surf. Sci. (in press).
12. For a recent review see S. A. Adelman and J. D. Doll, Accts. Chem. Res. (in press).
13. R. F. Wallis, Prog. Surf. Sci. 4, part 3 (1973).
14. A. J. Bennett, B. McCarroll, and R. P. Messmer, Surf. Sci. 24, 191 (1971).
15. M. R. Hayns, Theoret. Chim. Acta. (Berl) 39, 61 (1975).
16. J. H. McCreery and G. Wolken, Jr., Chem. Phys. Letters 46, 469 (1977).
17. J. T. Tou and R. C. Gonzalez, "Pattern Recognition Principles" (Addison-Wesley, Reading, 1974).
18. W. W. Bledsoe and I. Browing, Proc. East. Joint Comp. Conf., December, 1959, pp. 225-232.
19. Y. W. Lin, S. A. Adelman, and G. Wolken, Jr., Surf. Sci. 66, 376 (1977).

klt



TABLE I  
Parameters Used in Generating the Various Potentials

Potential	$\epsilon$	$Z_m$	$\delta$	$D_0$	$k$	$A$	$B$	$\Delta_1$	$\Delta_2 = \Delta_3$	1CN	2CN	5CN
I	1.0	3.12	1.0	0.1102	0.0	0.1067	0.2051	0.147	0.03	3.0	3.0	1.72
II	0.2112	2.19	0.0474	0.1007	1.0	1.463	0.653	0.147	0.03	3.0	2.74	1.72
III	0.2112	2.19	0.0474	0.1007	1.0	0.1463	0.653	-0.1	-0.1	3.0	2.74	2.40
IV	1.0	3.12	1.0	0.0551	0.0	0.1067	0.2051	0.147	0.03	1.5	1.5	0.86
V	1.0	3.12	1.0	0.0551	0.0	0.1067	0.2051	0.3	0.3	1.5	1.5	0.86
VI	0.2112	2.19	0.0474	0.0503	1.0	1.463	0.653	0.147	0.03	1.5	1.37	0.86
VII	1.0	3.12	1.0	0.0551	0.0	0.1067	0.2051	0.0	-0.3	1.5	1.5	0.86
VIII	1.0	3.12	1.0	0.0551	0.0	0.1067	0.2051	0.147	0.3	1.5	1.5	0.86
IX	0.2112	2.19	-0.1861	0.0503	1.0	-0.3725	0.653	0.147	0.03	0.86	1.37	1.5

TABLE II

Mean Distribution of Energy in Product Molecules

Potential	% Molecule Formation	% E <sub>vib</sub>	% E <sub>rot</sub>	% E <sub>trans</sub>
(a) Equal Masses				
IV	33	43	15	42
V	35	57	23	20
VI	33	50	10	40
VIII	29	61	20	19
IX	32	49	5	46
(b) Light-Heavy Mass Combination				
IV	24	46	12	42
V	39	44	34	22
VI	37	52	13	35
VIII	26	45	32	23
IX	40	30	20	50

TABLE III

Product Vibrational State Distribution  
(%) Summed Over Rotational Sublevels

Potential	v =	0	1	2	3	4	5
(a) Equal Masses							
IV		18	39	30	12	1	0
V		11	17	36	34	3	0
VI		8	36	39	15	2	0
VIII		1	20	48	26	5	0
IX		14	29	32	24	1	0
(b) Light-Heavy Mass Combination							
IV		11	20	20	30	15	4
V		15	21	26	22	7	9
VI		10	10	23	23	25	10
VIII		18	23	13	13	27	8
IX		39	22	14	20	3	2



TABLE IV

Mean Distribution of Energy in Product Molecules:  
a) rigid surface; b) 2 surface atoms free to move

Potential		% Molecule Formation	% E <sub>vib</sub>	% E <sub>rot</sub>	% E <sub>trans</sub>	% Energy Transfer
(a) Equal Masses						
IV	a)	41	41	15	44	
	b)	72	49	11	34	6.32
V	a)	36	60	20	20	
	b)	78	52	26	15	6.69
VI	a)	42	51	10	39	
	b)	65	57	8	30	5.24
VIII	a)	30	68	18	14	
	b)	69	62	18	13	7.04
(b) Light-Heavy Mass Combination						
IV	a)	21	47	13	40	
	b)	73	51	10	34	4.79
V	a)	40	49	30	21	
	b)	79	37	40	19	3.86
VI	a)	40	51	13	36	
	b)	69	47	17	32	5.89
VIII	a)	26	37	40	23	
	b)	70	46	27	23	4.26

TABLE V

Binding energies (in eV) and equilibrium heights above the surface (in Å) for atoms at different sites on the graphite surface.

	Bridge	On-Top	Hole
<u>H-Graphite</u>			
Energy	0.85	0.82	0.11
Distance	1.0	1.2	0.5
<u>O-Graphite</u>			
Energy	2.59	1.82	1.09
Distance	1.2	1.5	1.0
<u>C-Graphite</u>			
Energy	4.08	4.52	6.53
Distance	1.2	1.3	0.6

TABLE VI

Parameter values (in a.u.) for atom-graphite interactions.

	H-Graphite	O-Graphite	C-Graphite
a	0.0244	0.0814	0.1846
b	-0.0068	-0.0138	0.0185
c	0.0011	-0.0442	-0.0370
d	1.6535	2.2393	2.0790
e	-0.2362	-0.1228	-0.2830
f	0.7770	0.7937	0.4610



TABLE VII

Morse parameters (in a.u.) for the H-H interaction.

---

---

$D_0$	0.1744
$\alpha$	1.0277
$r_0$	1.4016

---

---

FIGURE CAPTIONS (all distances are given in a.u.)

1. Geometry of the W(001) surface indicating the singly coordinated (1CN) adsorption site and the 2CN, 5CN sites. The origin of coordinates is at a 1CN site with the x-y plane parallel to the surface and the x-axis directed towards a neighboring 1CN site. To study recombination dynamics, two atoms are given random initial momenta, subject to the restriction that the (x,y) components of momenta lie within the square indicated. This neglects "catch-up" collisions. 'a' = 5.97 a.u.
2. Equipotential contours (in eV) for the approach of H<sub>2</sub> to W(001) for the different potential surfaces studied. The contour levels are equally spaced for any given potential surface. The H-H bond is parallel to the plane of the surface. The center of mass of the molecule is perpendicularly above a 2CN site. X indicates the position of the reactants, 2 atoms adsorbed at adjacent 1CN sites (5CN for IX). • locates our choice of the "transition site".
3. Energy profiles along the reaction paths for the potential surfaces given in Figure 2. The dashed line marks the region of transition from reagents to products (denoted by • in Figure 2).
4. Basal plane of graphite; s = 2.68 a.u. The on-top (A), bridge (B), and hole (C) sites for an atom above the surface are indicated.
5. Equipotential contours (in eV) for an atom approaching surface of graphite in (X,Z) plane as defined in Figure 4 (y=0.0) (a) H atom, (b) O atom, (c) C atom.
6. Equipotential contours (in eV) for an atom in the (X,Y) plane of Figure 4 (a) H (Z=1.9), (b) O (Z=2.4), (c) C (Z=1.8).
7. Equipotential contours (in eV) for H<sub>2</sub> approaching the graphite surface in Figure 4. The H<sub>2</sub> bond is held parallel to the surface and the bond midpoint is fixed over site "A" (7A), site "B" (7B), site "C" (7C).

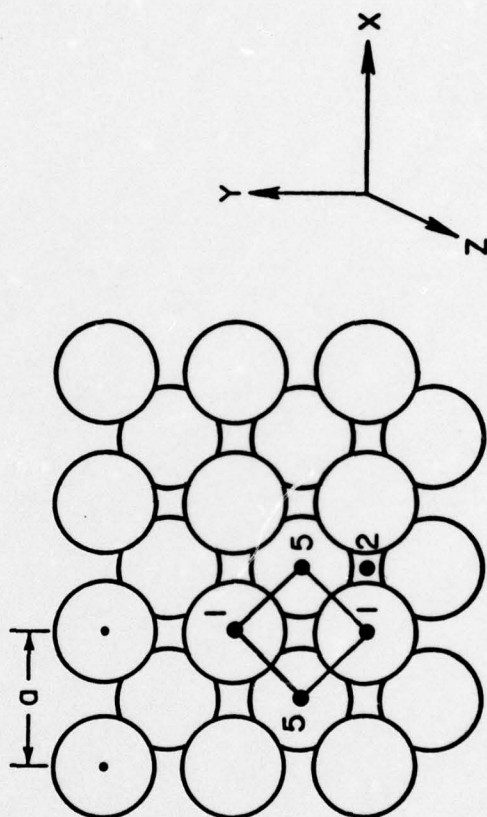


Fig. 1



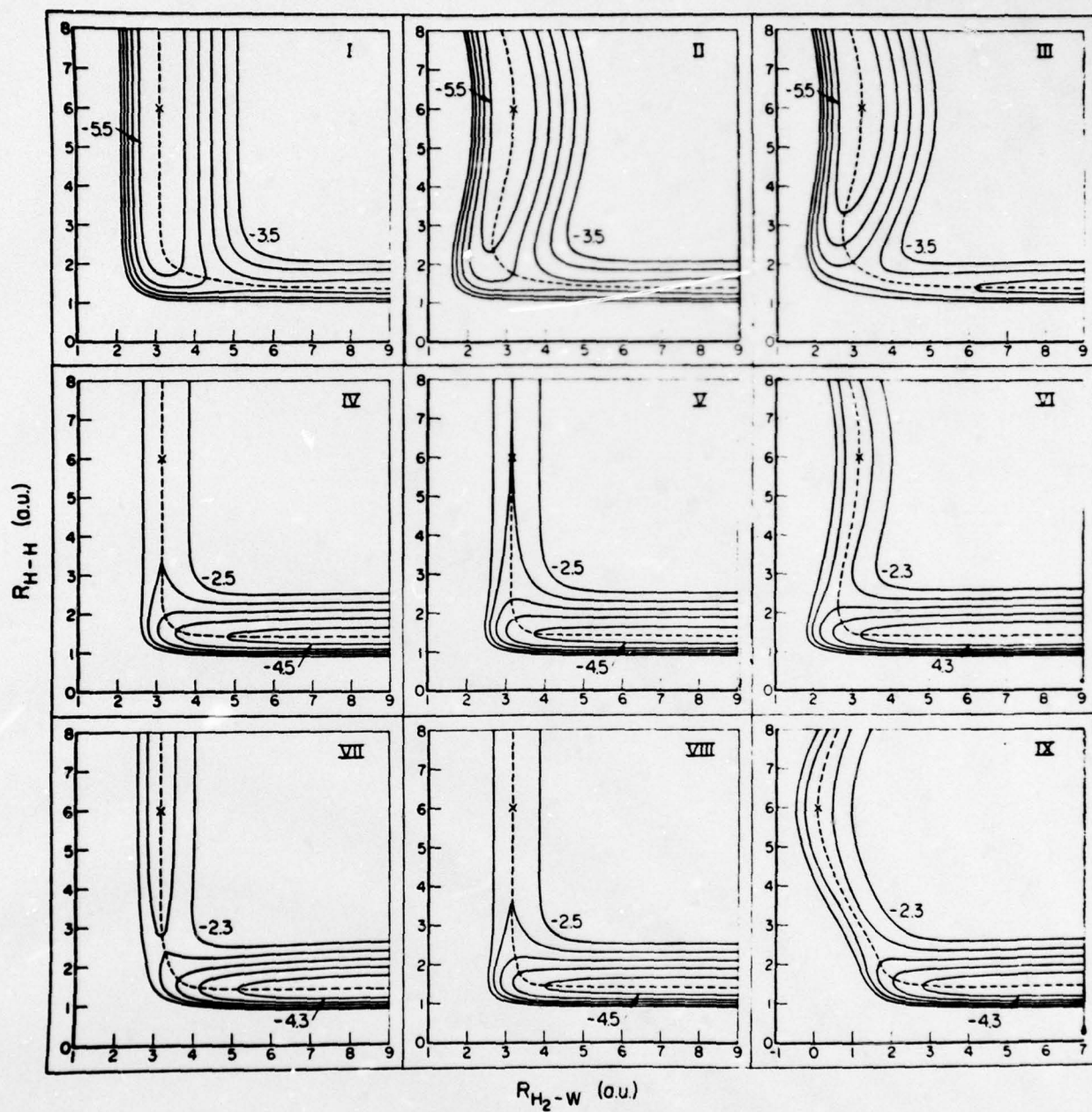


Fig. 2

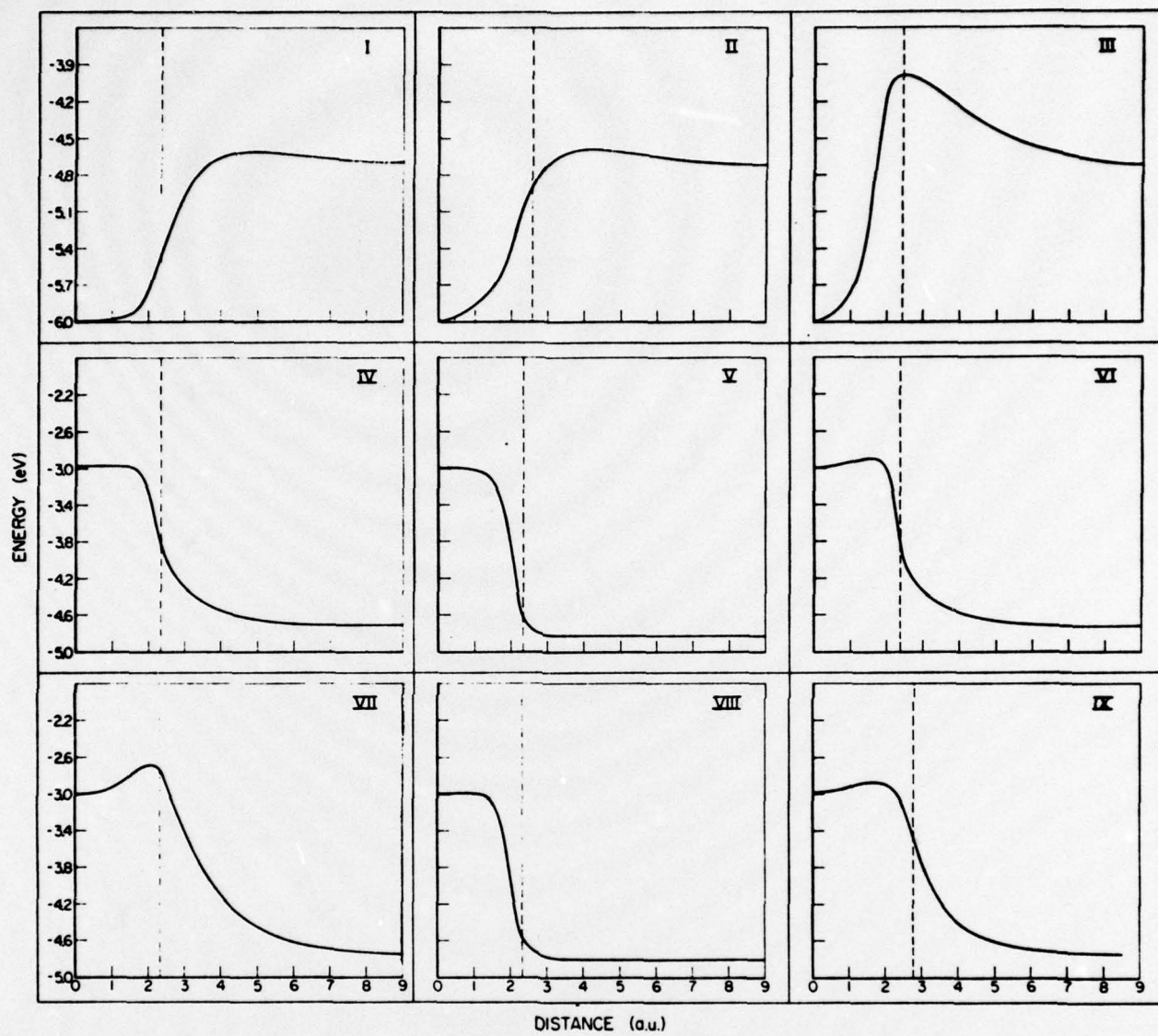


Fig. 3

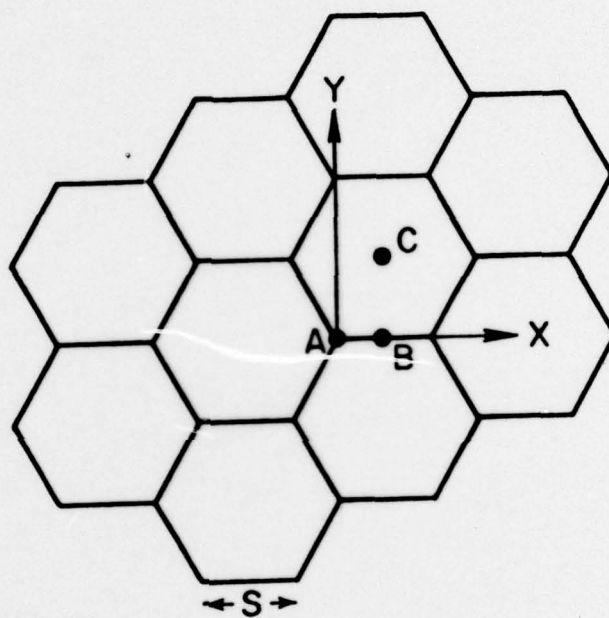


Fig. 4



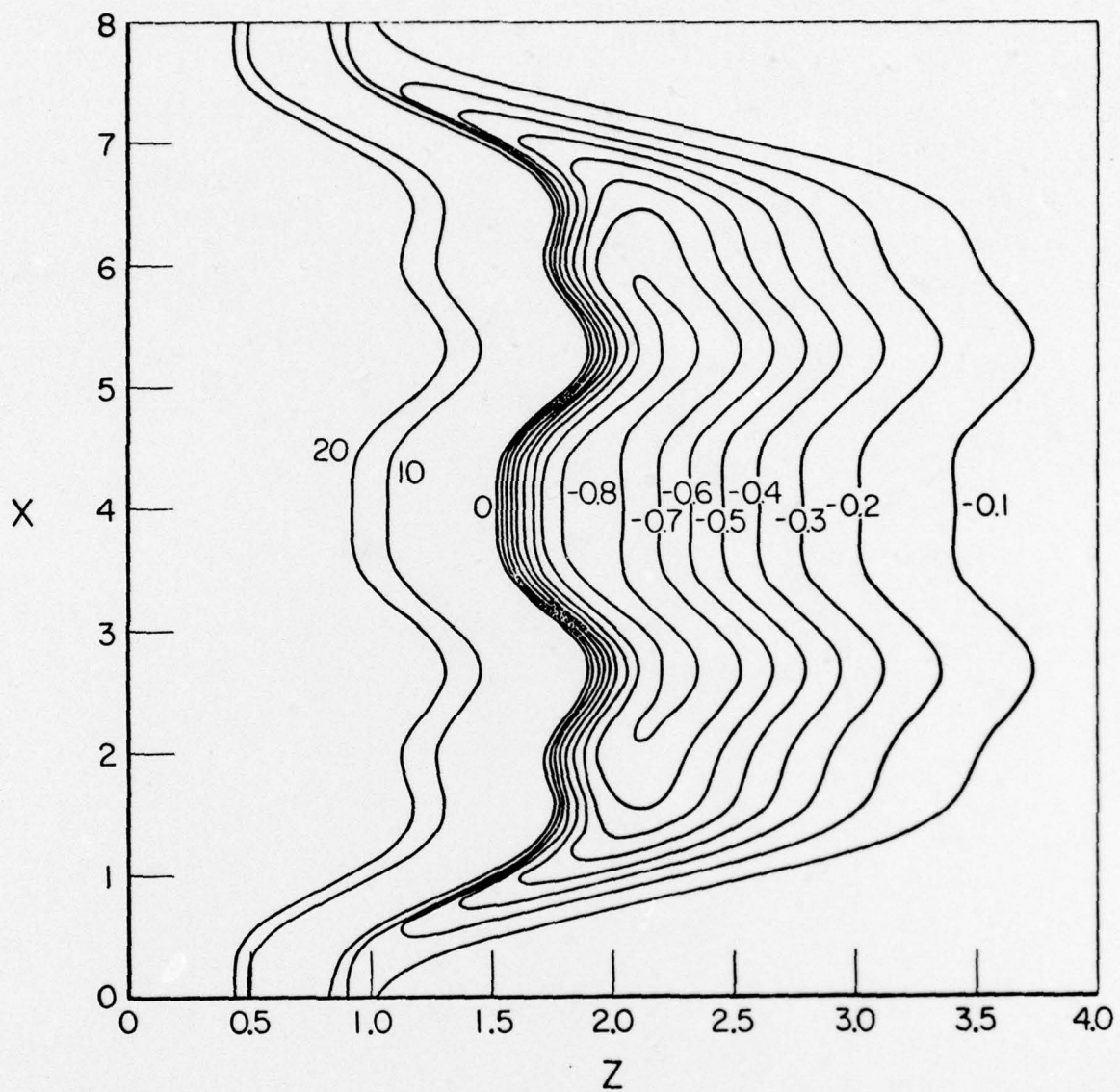


Fig. 5a

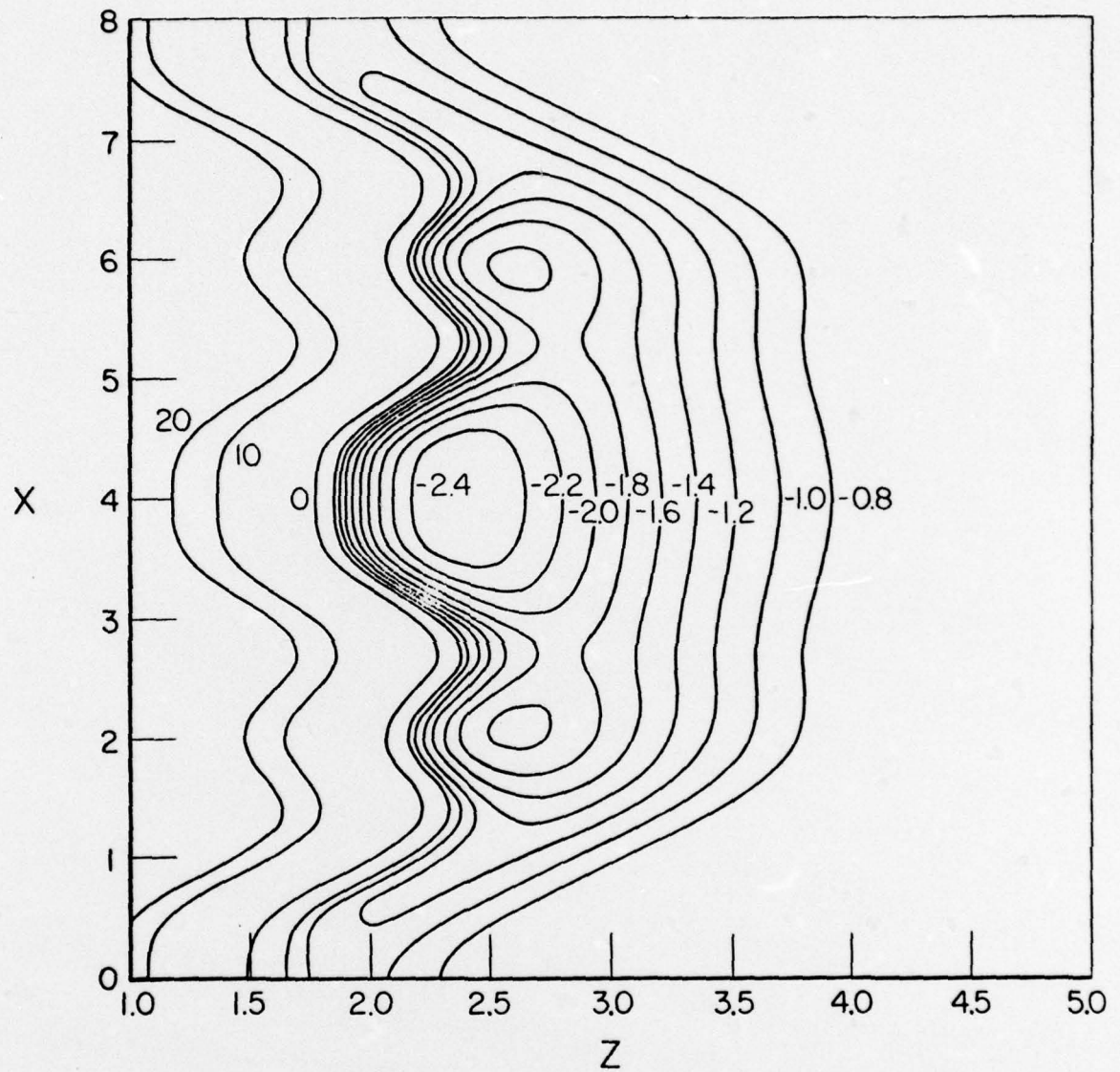


Fig. 5b

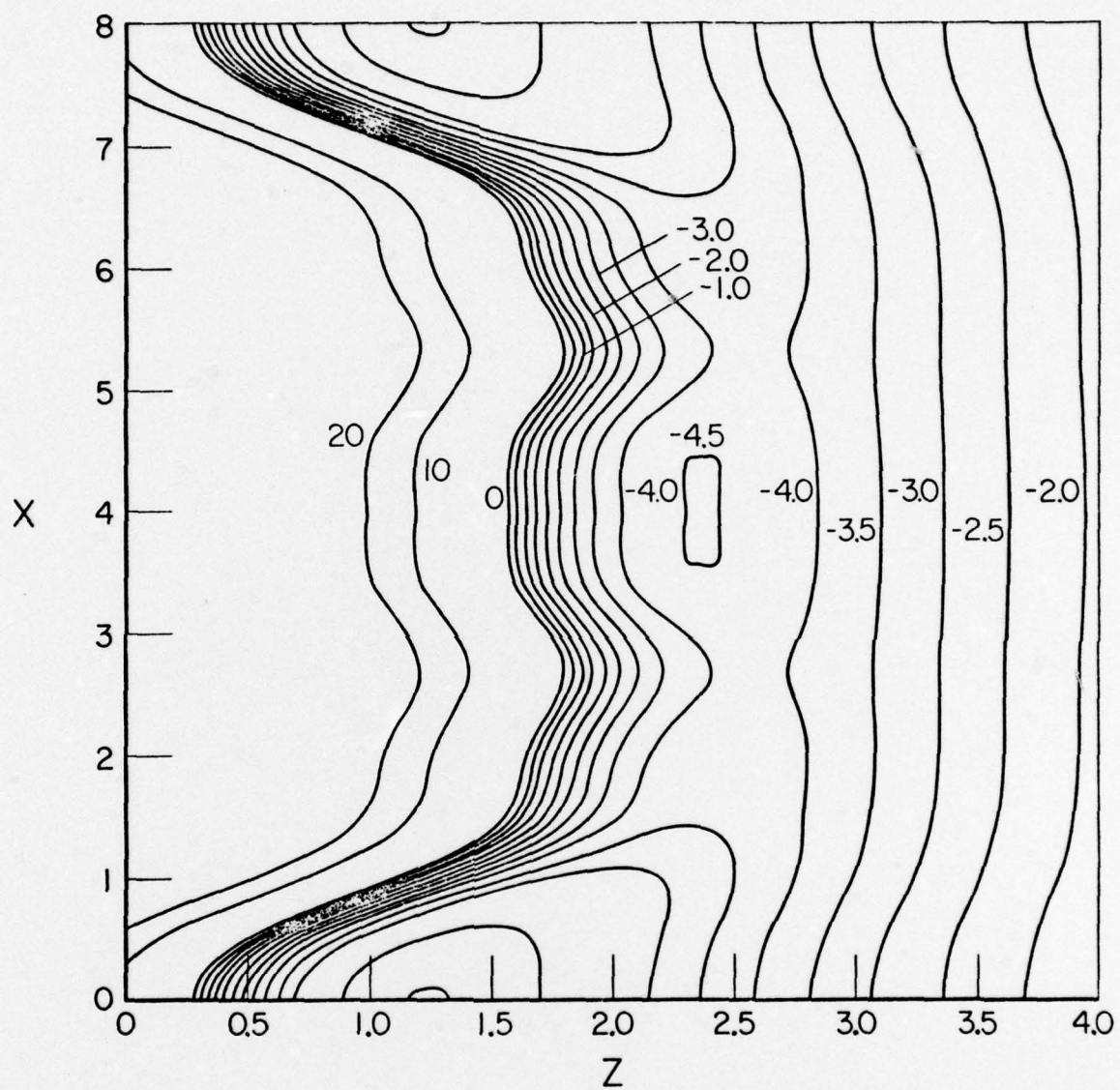


Fig. 5c



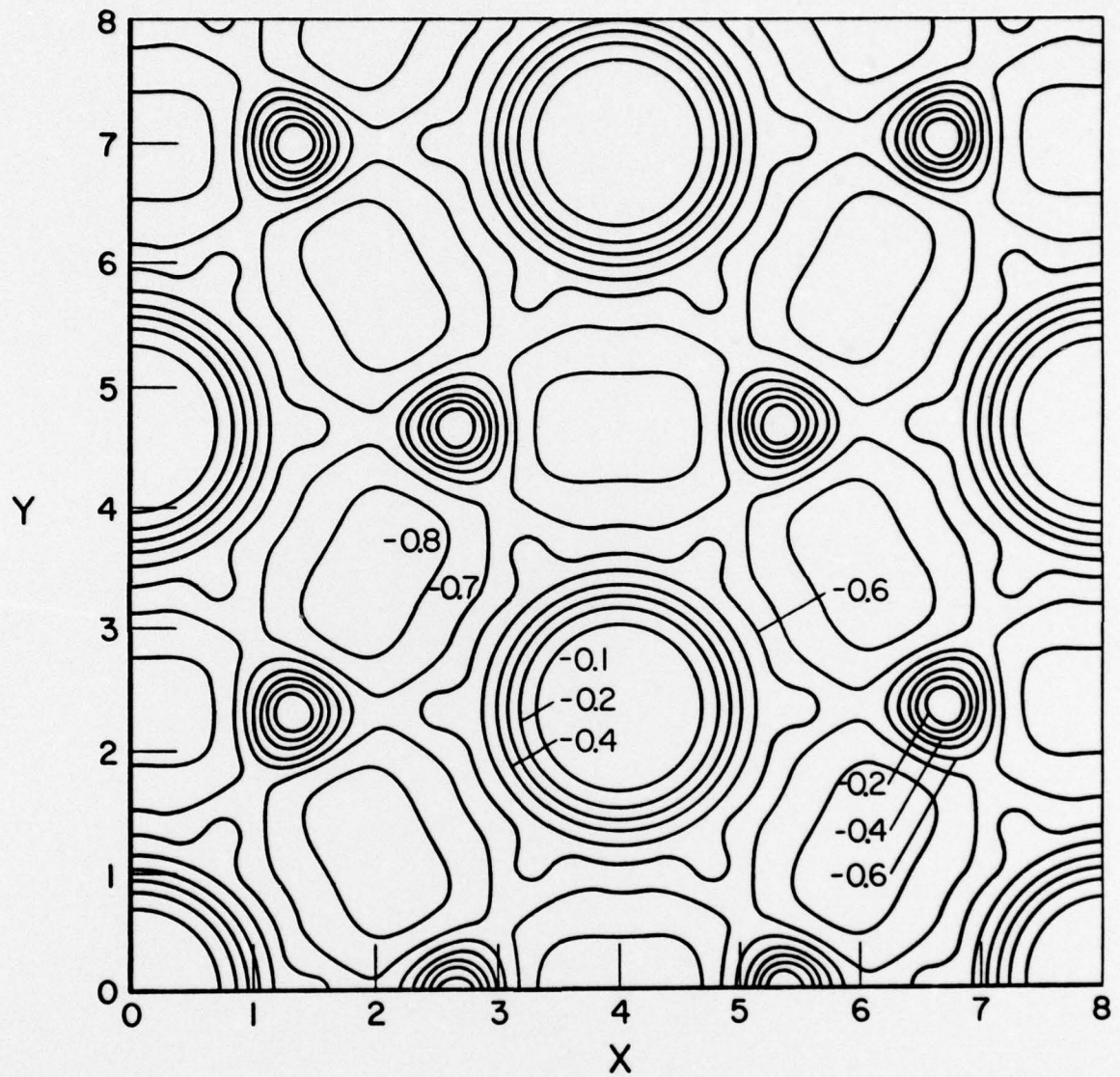


Fig. 6a

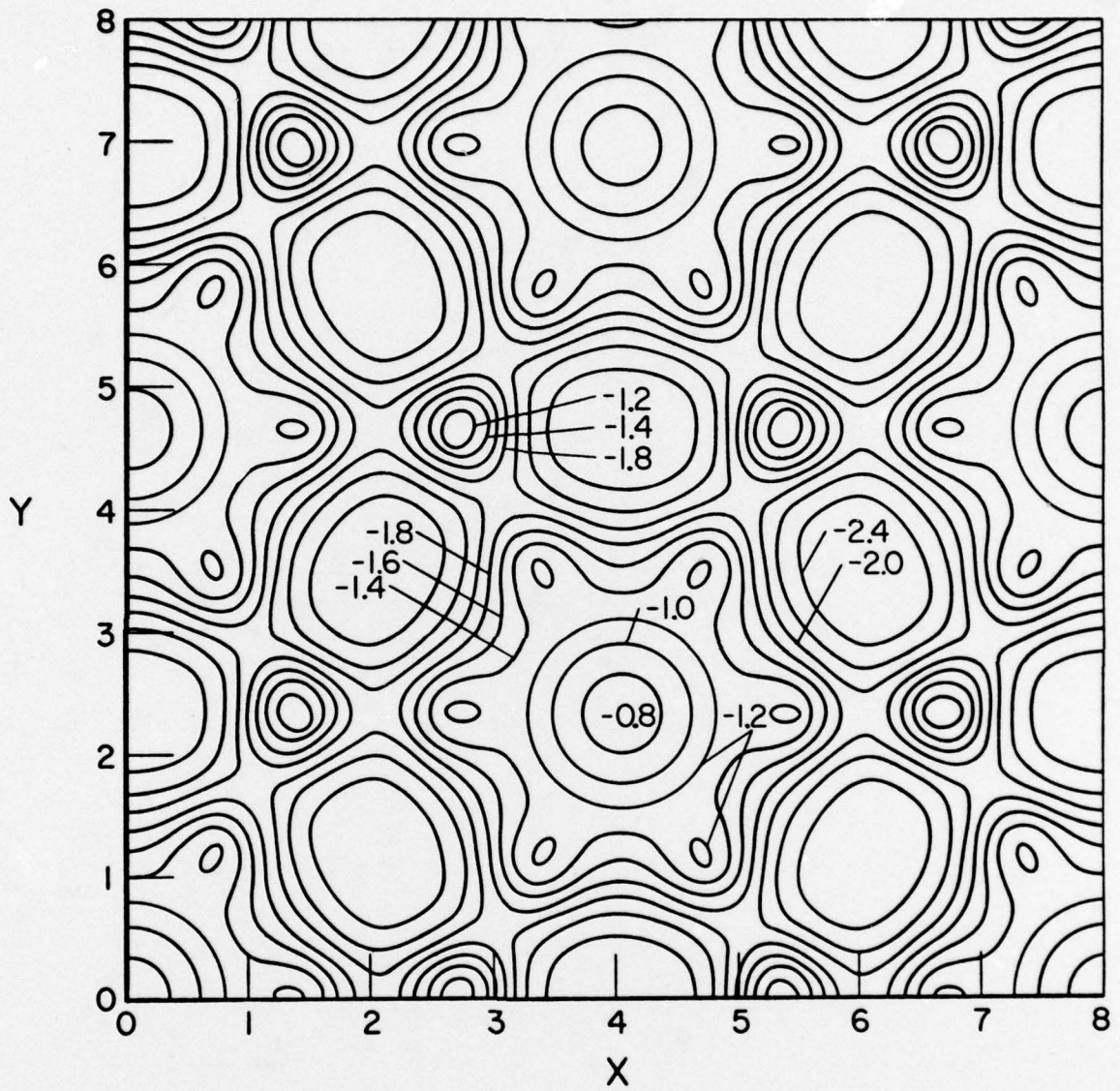


Fig. 6b

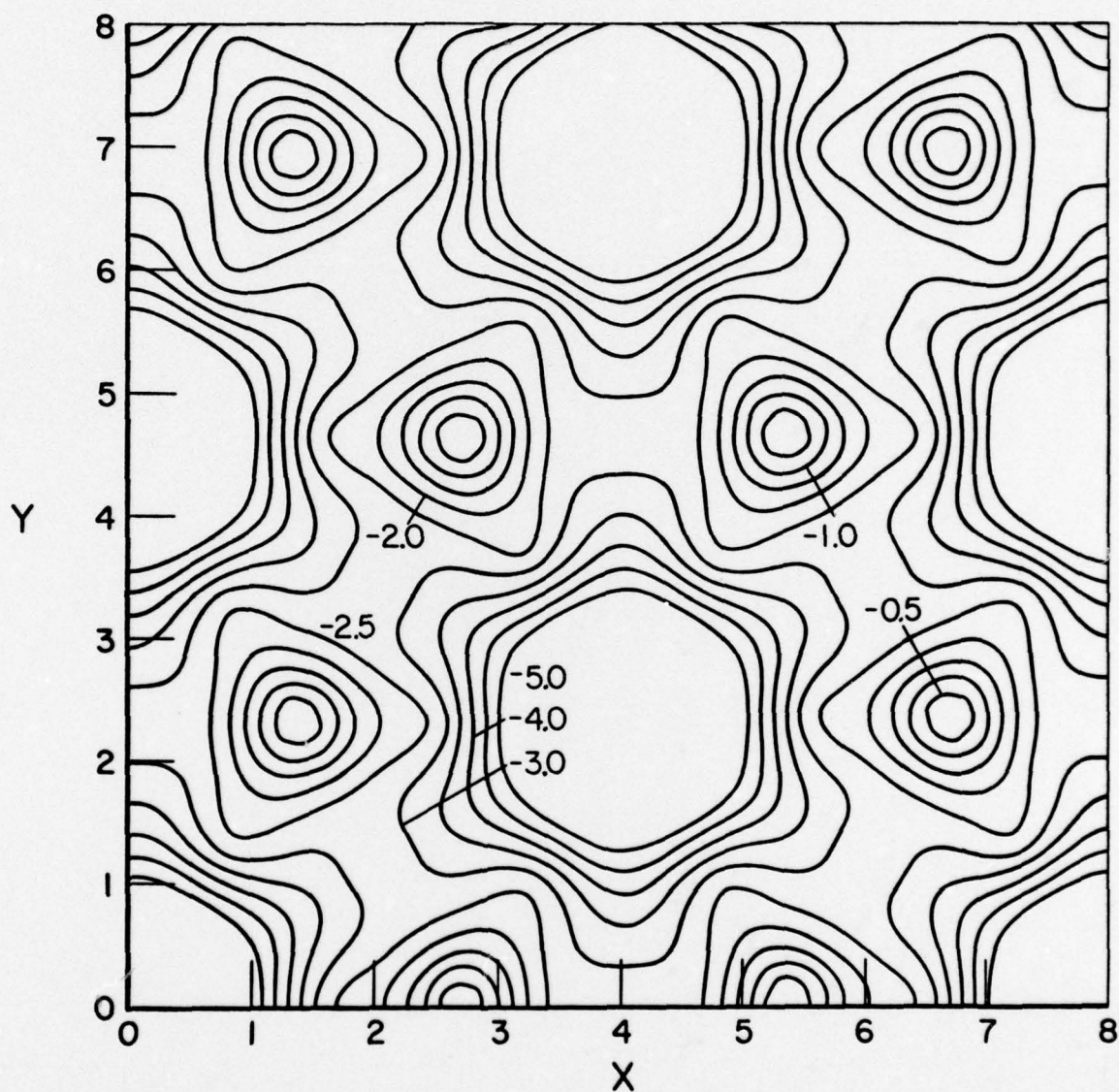


Fig. 6c



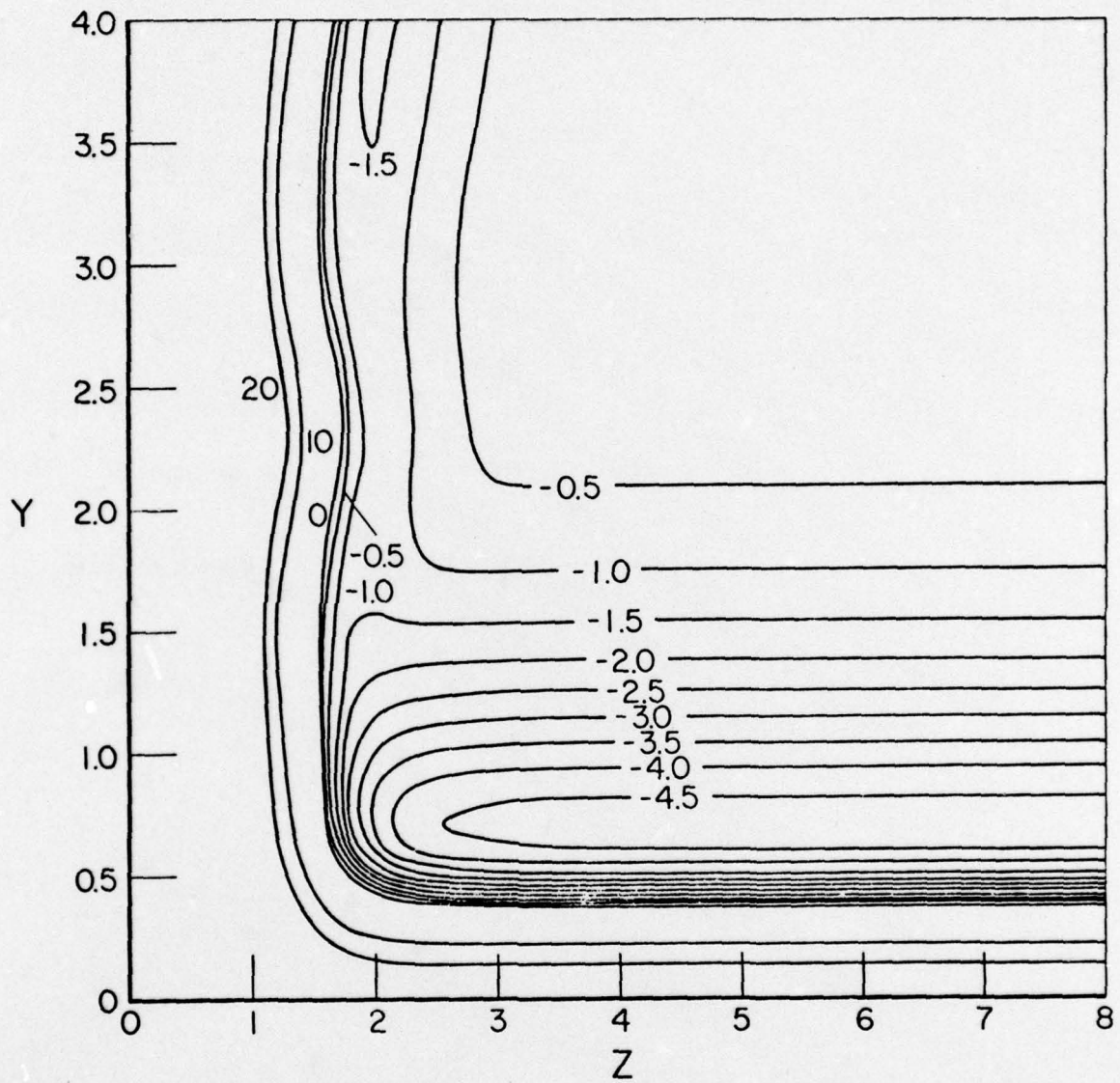


Fig. 7a

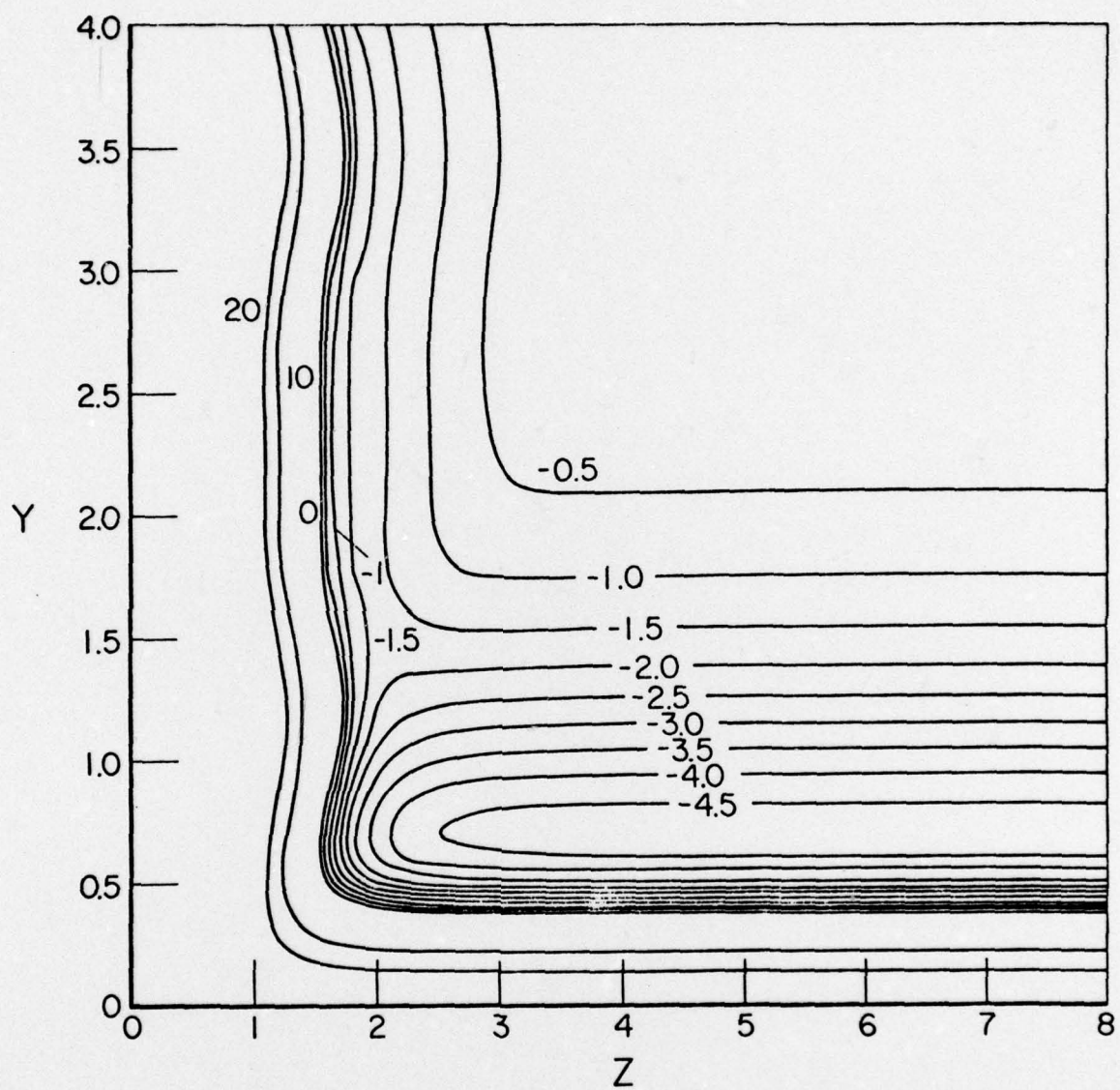


Fig. 7b

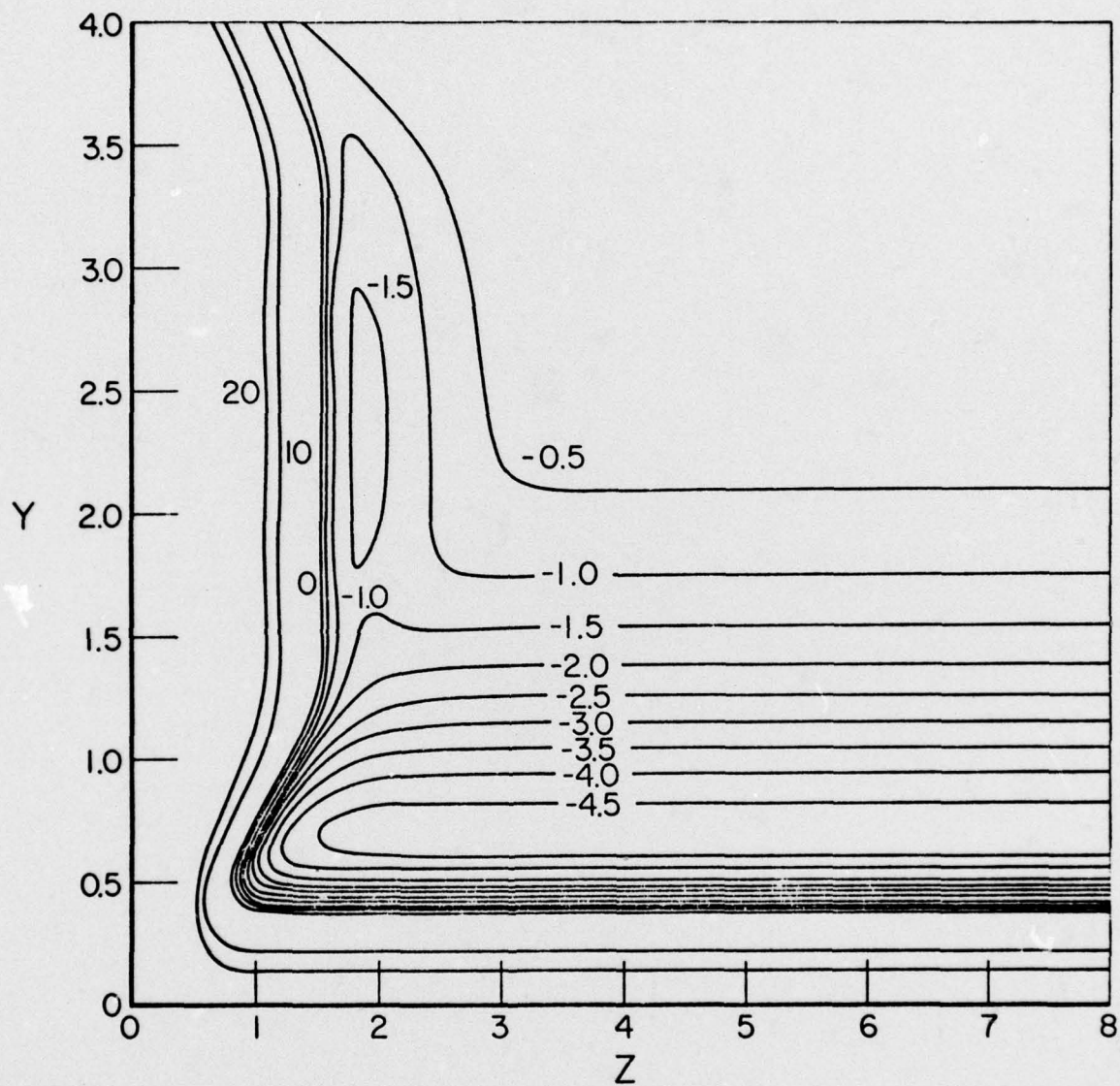


Fig. 7c